Available online at www.eccomasproceedia.org
Eccomas Proceedia COMPDYN (2025) 2589-2599

ECCOMAS
Proceedia

COMPDYN 2025
10th ECCOMAS Thematic Conference on
Computational Methods in Structural Dynamics and Earthquake Engineering
M. Papadrakakis, M. Fragiadakis (eds.)
Rhodes Island, Greece, 15-18 June 2025

LOW-FIDELITY NONLINEAR MODEL FOR THE SEISMIC ANALYSIS OF STRUCTURE-SOIL-STRUCTURE INTERACTION

Felipe Vicencio[1], **Christian Málaga-Chuquitaype**[2]

[1] Assistant Professor, Facultad de Ingeniería, Universidad San Sebastián
Bellavista 7, Recoleta, Santiago, Chile
e-mail: felipe.vicencio@uss.cl

[2] Associate Professor, Department of Civil and Environmental Engineering, Imperial College London
Skempton Building, London, UK.
c.malaga@imperial.ac.uk

Abstract

Analytical methods using reduced-order models with a limited number of degrees-of-freedom (DOF) have been well recognized and effectively applied in the evaluation of the SSSI effects during the dynamic response of buildings. In these mechanical models, a small number of lumped masses, dashpots, and springs are employed. This study examines the effects of Structure-Soil-Structure Interaction (SSSI) on the seismic response of multiple yielding structures embedded in a linear elastic soil. A nonlinear phenomenological Bouc–Wen model is assumed for the buildings. This model can identify vulnerable structures and therefore help to reduce city-wide seismic risk, protect lives, and decrease repair costs after a severe earthquake. We employ 35 real ground motions, recorded from 8 events between 1971 and 2007 in different parts of the world. These records have differences in amplitude, duration, envelope shape, and power spectral content. The findings emphasize the important differences between nonlinear SSSI and nonlinear SSI for different configurations. Additional analyses identify the key demand parameters influencing resilience, providing a deeper understanding of uncertainties in SSSI performance during seismic events.

Keywords: Structures-Soil-Structure Interaction (SSSI), Nonlinear analysis, Earthquake Engineering.

Peer-review under responsibility of the organizing committee of COMPDYN 2025.
doi: 10.7712/120125.12593.25690

1 INTRODUCTION

Usually, buildings in urban areas are designed by considering the response of structures as singleton structures in isolation (i.e., a single structure with no neighboring structures or Soil-Structure Interaction, SSI [1–3]). However, the high density of buildings in cities inevitably results in the possibility of seismic interaction of adjacent buildings through the underlying or surrounding soil. This phenomenon is widely known as Structure-Soil-Structure Interaction (SSSI) and has been reported in different recent works [4–8], among others. These works indicate that there is a substantial, currently unquantified increase (or reduction) in seismic risk in densely packed urban areas.

The complexity of the multi-structural interaction problem comes from the variety of parameters involved (spatial distribution and orientation of buildings, dynamic characteristics of structures, soil properties, and seismic excitation, among others). Therefore, researchers have used different techniques to address his problem. For example, numerical methods are one of the most effective and multipurpose tools for studying complex linear and nonlinear problems. Finite Element Method (FEM), Boundary Elements Method (BEM) or a combination of these two FEM/BEM procedures has been widely used to assess SSSI problems [9–15]. These studies have identified important factors that control the seismic interaction behavior such as: (i) the separation building distance, (ii) the direction of the orientation between foundations, (iii) the height ratio and dynamic characteristics of adjacent buildings, (iv) the aspect ratio (the building height to width ratio), and (v) the soil type beneath the buildings. One clear advantage of using such methods is the possibility of modelling complex geometries and considering nonlinearities in the elements. However, those models have a large number of degrees of freedom, leading to computationally costly and time-consuming analyses.

Low-fidelity models, with a relatively limited number of degrees of freedom, have been well recognized and effectively applied in the evaluation of the SSSI effects on the dynamic response of buildings [16–20]. These models (i) capture the most important dynamic behavior, (ii) have a relatively small amount of system parameters and (iii) are computationally simple for exploring a vast number of generic cases. They are not meant to substitute advanced computational models and experimental work of specific cases.

Experimental methods (centrifuge tests and shaking table test) represent an important validation point for numerical models and provide preliminary estimates of the effects of complex interaction problems. For example, Trombetta et al. [21–23] performed six centrifuge experiments, where the inelastic structural response of two adjacent steel moment resisting frames was considered. Knapett et al. [24,25] analyzed similar and highly dissimilar building on shallow foundations using centrifuge modelling. Finally, Aldaikh et. al. [26,27] has indicated that the presence of neighboring buildings could produce favorable/detrimental changes in seismic response. These represent important validation points for numerical models and provide preliminary estimates of the effects of complex interaction problems.

Based on the previous discussion, this paper aims to introduce a mathematical formulation of the problem of SSSI, where the model enables the nonlinear behavior of the structure. We employ 35 real ground motions, recorded from 8 events between 1971 and 2007 in different parts of the world. The objective of this research is to answer the following two questions: (i) How significant is the SSSI problem on the seismic response in nonlinear buildings? and (ii) Is there evidence to suggest that different types of earthquakes can affect differently the SSSI behavior?

2 LOW-FIDELITY FORMULATION FOR SSSI FOCUSSES ON INELASTIC STRUCTURES

Considering the system shown in Figure 1. It comprises of a pair of buildings described in terms of four DOFs and coupled by a rotational ground spring κ. The soil/foundation system of each building has one rotational DOF at the foundation level θ_j. The building super-structures have one translational DOF relative to the ground (x_j). Thus, the two DOFs of each building can be viewed as a projection, onto a two modes vector basis of a generalised building. A known ground displacement field x_g is applied at both foundations, i.e. wave passage effects and spatially heterogeneous ground displacement are neglected in the present work. h_j is the total height of the buildings, m_{bj} is the total lumped modal mass of the buildings, m_s is the foundation/soil mass underneath the buildings, with $j \in [1,2]$. k_{bj} is the elastic modal horizontal stiffness of the structure. k_s is the rotational stiffness of the soil/foundation, and b is the foundation width. F_{bj} are the restoring nonlinear force related to the initial lateral stiffness of the buildings.

The kinetic energy and potential energy for this system are given by the equations (1) and (2), respectively.

$$T_E = \frac{1}{2}\sum_{j=1}^{2} m_{bj}\left(\dot{x}_j + \dot{x}_g - h_j\dot{\theta}_j\right)^2 + m_s r^2 \dot{\theta}_{sj} \tag{1}$$

$$U_E = \frac{1}{2}\sum_{j=1}^{2}\left(2\int F_{bj}dx_j + k_s\theta_{sj}^2\right) + \frac{1}{2}\kappa(\theta_2 - \theta_1)^2 \tag{2}$$

The equation of motion of the complete dynamic system can be derived using the Euler-Lagrange equations as follows.

$$\mathbf{M\ddot{u}} + \mathbf{C\dot{u}} + \mathbf{Ku} + \mathbf{F} = \mathbf{p}\ddot{x}_g \tag{3}$$

where system matrices are defined as follows,

$$\mathbf{M} = \begin{bmatrix} m_{b1} & -m_{b1}h_1 & 0 & 0 \\ -m_{b1}h_1 & m_{b1}h_1^2 + m_s r^2 & 0 & 0 \\ 0 & 0 & m_{b2} & -m_{b2}h_2 \\ 0 & 0 & -m_{b2}h_2 & m_{b2}h_2^2 + m_s r^2 \end{bmatrix}, \mathbf{F} = \begin{bmatrix} F_{b1}(x_1) \\ 0 \\ F_{b2}(x_2) \\ 0 \end{bmatrix} \tag{4}$$

$$\mathbf{K} = \begin{bmatrix} 0 & 0 & 0 & 0 \\ 0 & k_s + \kappa & 0 & -\kappa \\ 0 & 0 & 0 & 0 \\ 0 & -\kappa & 0 & k_s + \kappa \end{bmatrix}, \mathbf{p} = \begin{bmatrix} -m_{b1} \\ m_{b1}h_1 \\ -m_{b2} \\ m_{b2}h_2 \end{bmatrix}, \mathbf{x} = \begin{bmatrix} x_1 \\ \theta_1 \\ x_2 \\ \theta_2 \end{bmatrix} \tag{5}$$

The nonlinear behavior of the buildings is considered by means of the Bouc-Wen hysteretic model, where the restoring nonlinear force associate to each building is defined as,

$$F_{bj} = Ak_{bj}x_j + (1 - A)k_{bj}x_{yj}z_j \tag{6}$$

where A is the post-yield to pre-yield ratio, x_{yj} is the yield displacement, and z_j is the Bouc-Wen hysteretic displacement parameter that obeys the following nonlinear differential equation.

$$\dot{z}_j = \frac{\dot{x}_j}{x_{yj}} \frac{\left[1 - \nu(E_{bj})|z_j|^n \{\beta + \gamma \text{sgn}(\dot{x}_j z_j)\}\right]}{\eta(E_{bj})} \quad \textbf{(7)}$$

The system's linear viscous damping matrix $\mathbf{C}$, defined in equation (3), assumes that each natural mode $n \in [1,6]$ is damped at $\xi_n = 0.05$ of critical damping. $\boldsymbol{\phi}_n$ is the eigenvector for mode n, ω_n are the natural frequencies of the systems. Thus, the Caughey orthogonal damping matrix $\mathbf{C}$ can be calculated as [21]:

$$\mathbf{C} = \mathbf{M}\left(\sum_{n=1}^{6} \frac{2\xi_n \omega_n}{\boldsymbol{\phi}_n^T \mathbf{M} \boldsymbol{\phi}_n} \boldsymbol{\phi}_n \boldsymbol{\phi}_n^T\right)\mathbf{M} \quad \textbf{(8)}$$

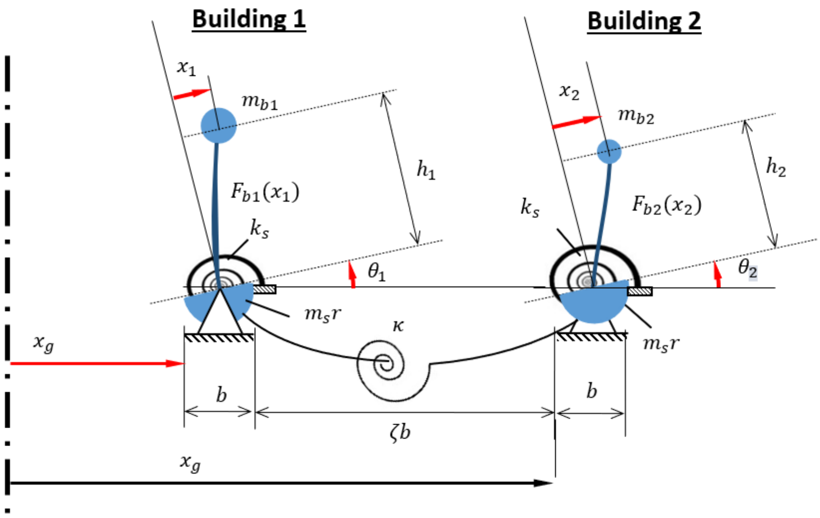

Figure 1: Structural model.

The scope of this analysis is restricted to a special case, by assuming the following.

- The same soil profile (loose sand with an average soil density of $\rho_s = 1300 kg/m^3$) exists under both buildings, this means that the rotational stiffness of the soil/foundation of buildings 1 and 2 are the same, k_s..
- Both buildings have a similar square plan area of $b = b_1 = b_2$.
- The buildings can be of different heights h_j, where the first building frequency is estimated using the approximation of Eurocode 8 EN-1998 for the natural period of a structure on a rigid foundation as $T_x = C_t h_1^{3/4}$ with $C_t = 0.075$.
- The frequency ratio between buildings 1 and 2 is defined as $\Omega_b = \omega_{b1}/\omega_{b2}$ (Different works use the height ratio $\varepsilon = h_2/h_1$, which can be considered as an equivalent parameter).
- The aspect ratio for building 1 is defined as $s = h_1/b$.
- The yield displacements are given by the terms x_{yj} and the yield loads $F_{byj} = k_{bj} x_{yj} \approx \Gamma m_{bj} S_d(T_x)$, where $S_d(T_x)$ is the elastic design spectrum ordinate from Eurocode 8, Part 1, and $\Gamma = 2.0$ accounts for the contribution of the gravity load (assuming 2.0 based on portal frame).
- The buildings are spaced at some arbitrary distance zb from each other.

- Building pounding is not permitted as inter-building spacing is assumed large enough to avoid it.

3 RESULTS AND DISCUSION

3.1 Ground motion selection

To calculate the effect of SSSI on the system we consider three types of ground motion. These include Far-Field (FF), Near-Field Without Pulse (NFWP) and Near-Field Pulse-Like (NFPL) record sets. The ground motions database is obtained from FEMA P695. The recorded acceleration series of these ground motions are selected from the Pacific Earthquake Engineering Research (PEER-NGA) West database. The FEMA P695 recommends a set of 22 FF records that are taken from 14 events that occurred between 1971 and 1999. Eight of them occurred in California, and six of them are taken from different places around the world. Each record has two horizontal components. Event magnitudes range from $M_w = 6.5$ to $M_w = 7.6$ with an average magnitude of $M_w = 7.0$. Values of their peak ground accelerations (PGAs) vary from 0.21g to 0.82g with a mean value of 0.43g. The next figure shows the elastic response spectra from all records set used in this research.

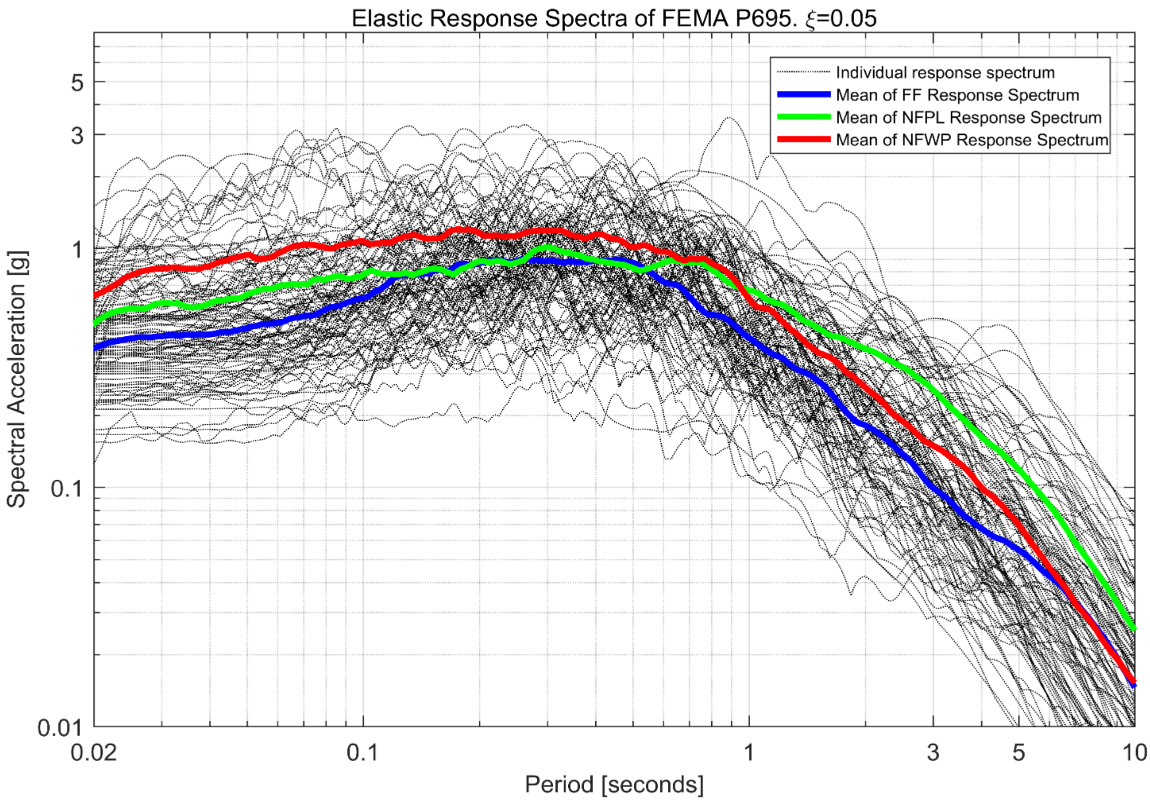

Figure 2: Elastic response spectra from FEMA P695 ground motions.

3.2 Response of the system for a set of parameters

In this section, we investigate the differences between nonlinear SSSI and SSI seismic responses. We examine the case when the building has a first natural period on a rigid foundation equal to $T_x = 0.5[s]$, frequency ratio $\Omega_b = \omega_{b1}/\omega_{b2} = 1.2$ (i.e., when the building 1 is neighbouring a 27.5[%] taller building), and building 1 has a height to width ratio equal to $s = h_1/b = 2$. The analysis is carried out first for the San Fernando (Carbon Canyon Dam station) earthquake as an example.

The percentage difference in the response total power $\ddot{\chi}_{bj}$ (for building j), when using the response SSSI-NL (Structure-Soil-Structure Interaction) rather than SSI-NL (Soil-Structure Interaction) is defined by the next equation,

$$\chi_{bj} = 100\left\{\frac{[E_s(U_{bj})]_{SSSI}}{[E_s(U_{bj})]_{SSI}} - 1\right\}, \quad \ddot{\chi}_{bj} = 100\left\{\frac{[E_s(A_{bj})]_{SSSI}}{[E_s(A_{bj})]_{SSI}} - 1\right\} \tag{9}$$

where $E_s(U_{bj})$ and $E_s(A_{bj})$ are the total power spectral density (based on all data points of response time series U_{bj} and A_{bj}) for the displacement and acceleration (referring to building "j"). The power spectral density (PSD) is defined using Parseval's theorem.

Figure 3(a) shows the coupled (SSSI, red line) and uncoupled (SSSI, blue line) nonlinear response for the top of building 1 (namely the displacement U_{b1} and the total acceleration A_{b1}). Comparing the responses, we observe that the larger displacement and acceleration are produced in the SSSI cases. The plot of the displacement (SSSI) shows an important asymmetric oscillation due to the nonlinear behavior, where there exists a large probability of the building coming to rest leaning at some angle at the end of the movement. Figure 3(b) depicts the corresponding power spectral density (PSD) for the displacement and total acceleration for building 1 considering the coupled and uncoupled cases. Comparing the SSSI and SSI responses, building 1 is affected by the taller building 2. There is a big amplification in the displacement and acceleration power spectral density for a Fourier frequency equal to 1.4 Hz (which represents building 1′s first natural frequency). The change in power is equal to $\chi_{b1} = 71\%$ for the displacement U_{b1}. So, the SSSI effect is larger when the nonlinear behaviour of the buildings is considered. On the other hand, in the case of the acceleration ($\ddot{\chi}_{b1} = 30\%$) the SSSI effects are less important.

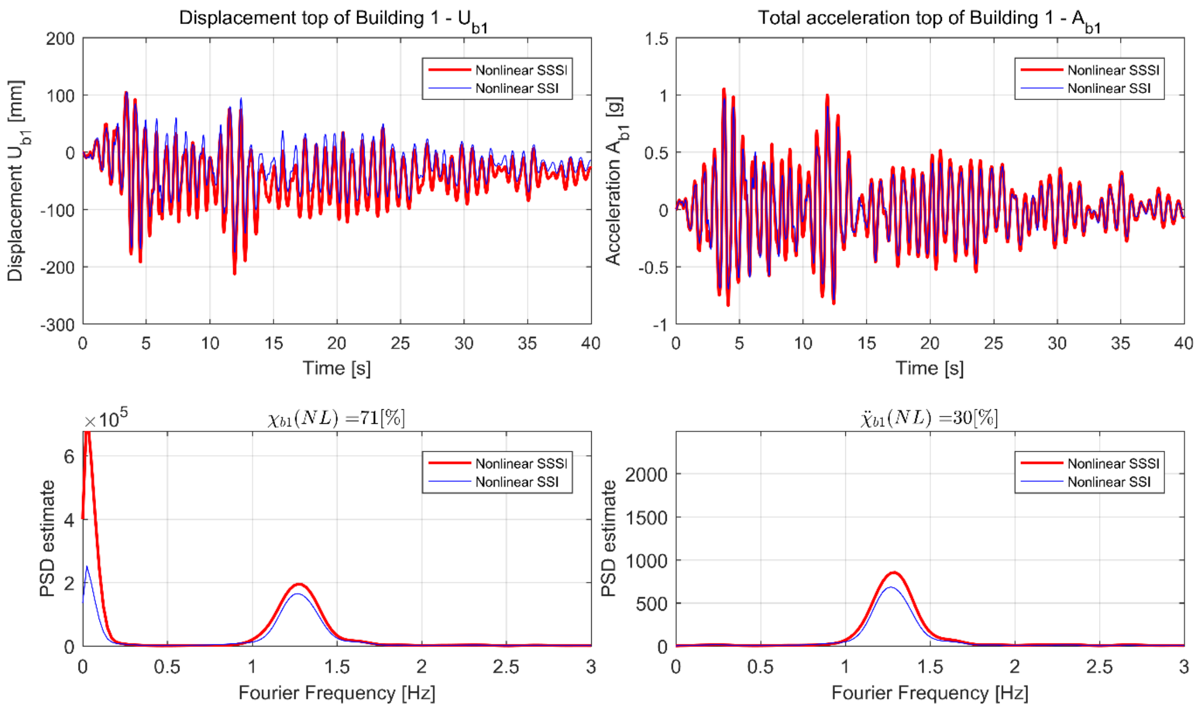

Figure 3: (a) Displacement and acceleration responses of building 1, (b) Power spectral density of displacement and acceleration response of building 1. San Fernando Earthquake.

Figure 4(a) shows the coupled (SSSI) and uncoupled (SSI) response at the top of building 2 (namely the displacement U_{b2} and the total acceleration A_{b2}). Figure 4(b) shows the corresponding power spectral density. There is a decrease in the seismic energy in building 2 which produces a reduction in the seismic response ($\chi_{b2} = -37\%$ in displacements U_{b2}, and $\ddot{\chi}_{b2} = -20\%$ in accelerations A_{b2}).

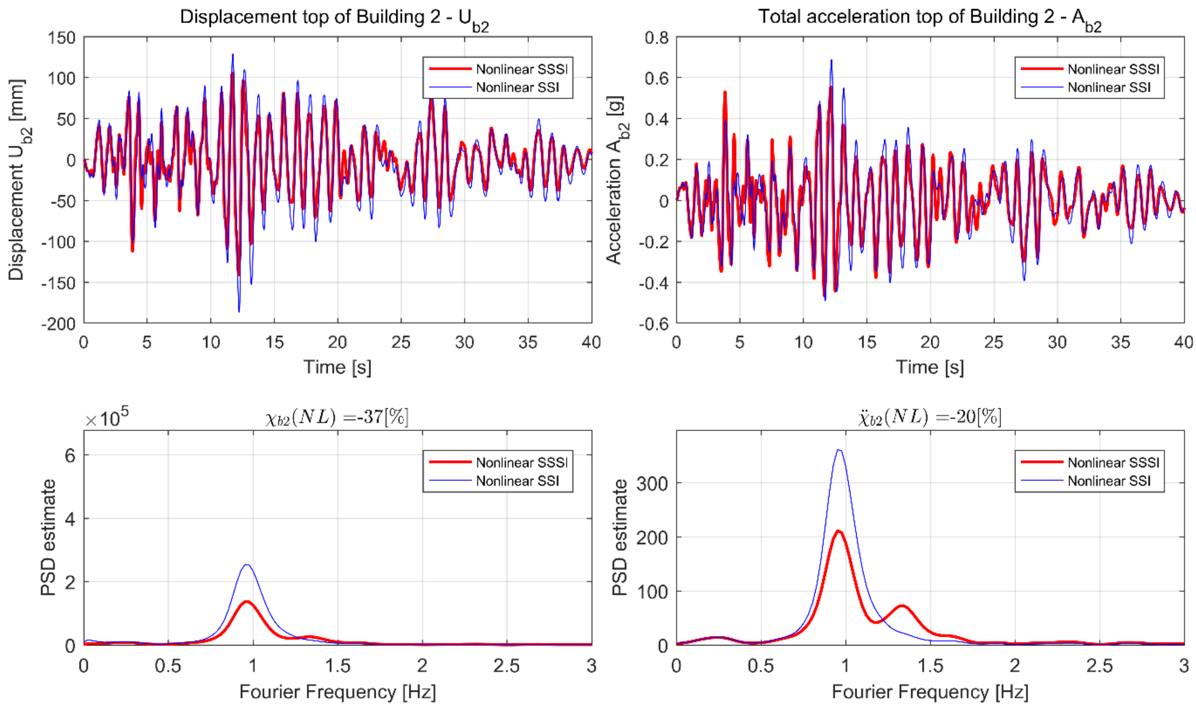

Figure 4: (a) Displacement and acceleration responses of building 2, (b) Power spectral density of displacement and acceleration response of building 2. San Fernando Earthquake.

Figure 5 displays the hysteresis cycles in buildings 1 under seismic action, computed by the Bouc-Wen formulation. As can be seen, there is an increase in non-linear behavior for the SSSI case.

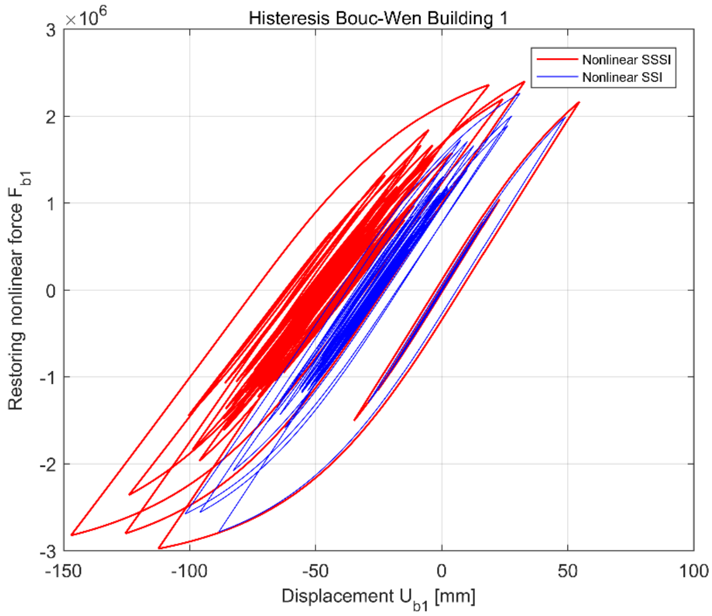

Figure 5: Hysteresis loops for building 1 (SSSI-NL and SSI-NL). San Fernando Earthquake.

3.3 Change in power with variation in aspect ratio and height ratio

We now turn to the change in power of building 1 (for the displacement χ_{b1} and acceleration $\ddot{\chi}_{b1}$). This term would be zero if there was no difference between the coupled (SSSI) and uncoupled (SSI) analyses. Presented in this section are results for the variation of change in power for buildings with aspect ratio $s = h_1/b$ varying between 0.25 and 4.0; frequency ratio between the buildings $\Omega_b = \omega_{b1}/\omega_{b2}$ varying between 0.5 and 2. The system is subjected to all the East-West and North-South components of earthquake records described above. The maximum, mean, and one standard deviation values of the change in power are presented.

Figure 6 shows the maximum, mean, and one standard deviation of the contour plots of variation of change in power χ_{b1} for the displacement U_{b1}. In this case, the maximum change in power lies around a frequency ratio equal to $\Omega_b = 1.1$ and larger values. The amplification reaches values of $\chi_{b1} = 150\%$, $\chi_{b1} = 20\%$ and $\chi_{b1} = 30\%$ for the maximum, mean, and one standard deviation, respectively.

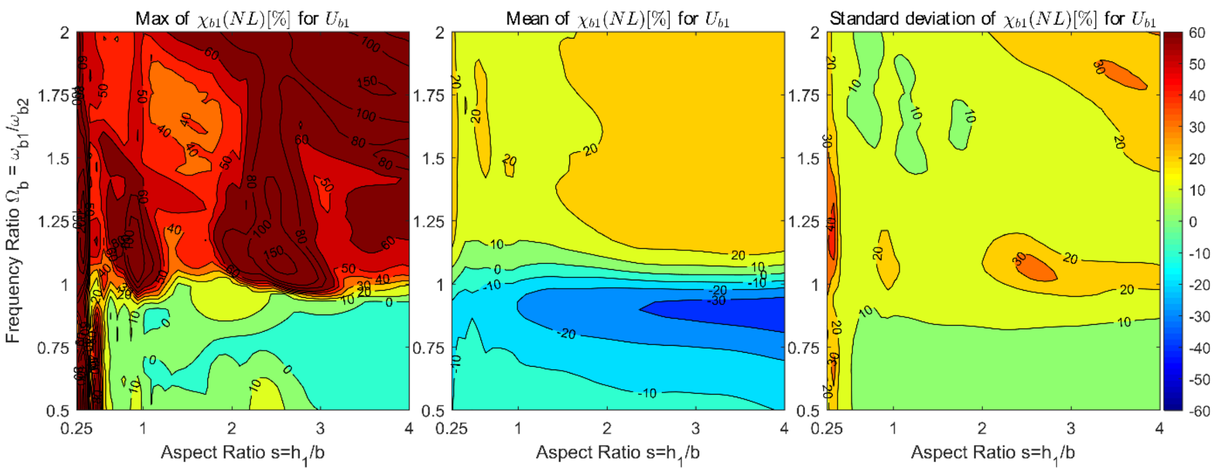

Figure 6: Maximum value, average, and standard deviation in change in displacement power χ_{b1}.

The maximum, mean and one standard deviation of the change in power $\ddot{\chi}_{b1}(NL)$ for the acceleration A_{b1} are shown in Figure 7. On average, the amplification of building 1's nonlinear total response reaches values of $\ddot{\chi}_{b1}(NL) = 40\%$, and the standard deviation reaches values of 30%.

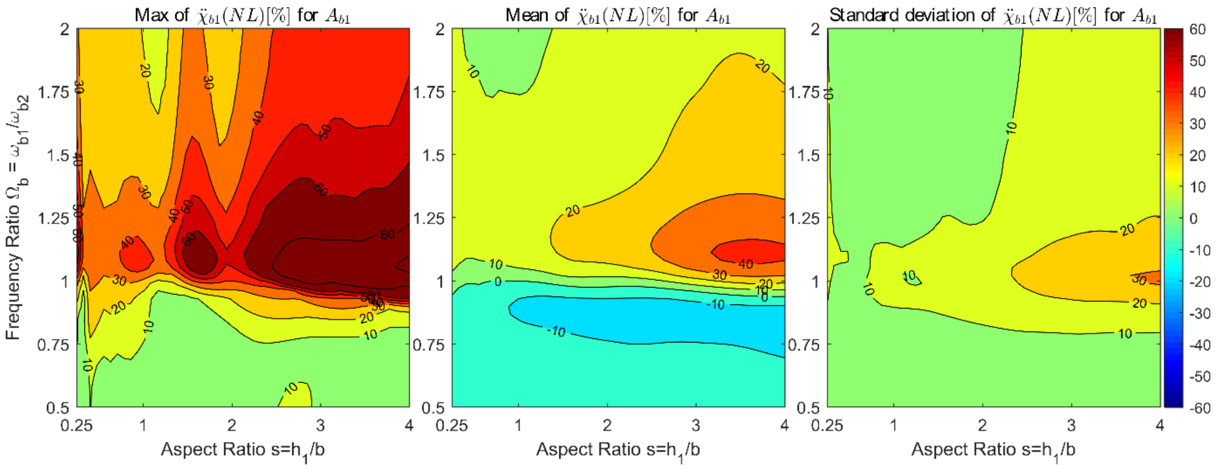

Figure 7: Maximum value, average, and standard deviation in change in acceleration power $\ddot{\chi}_{b1}$.

4 CONCLUSION

In this paper, we have presented a theoretical formulation for SSSI between two nonlinear buildings. These structures are coupled through the underlying soil. Three types of ground motion were considered (Far-Field, Near-Field Without Pulse and Near-Field Pulse-Like records sets), selected from FEMA P695. The analyses have been undertaken for loose soil. The research presented in this paper has led to the following principal findings:

- As a general trend, the SSSI effects on a nonlinear building adjacent to a smaller building produce amplifications of up to 20% in displacements and 40% in accelerations (mean for all earthquakes considered), i.e., the energy of the earthquake passes from the taller (and heavier) building to the smaller building.
- It is found that the most adverse interaction effect occurs when the nonlinear building 1 (shorter period) is adjacent to a more flexible building (longer period, $\Omega_b = \omega_{b1}/\omega_{b2} \approx 1.1$ and significant differences of height $\Omega_b > 1.75$).
- For some earthquakes an important amplification in the change of power, especially for the displacement, was observed.

5 ACKNOWLEDGEMENTS

The first author is grateful to the Ministry of Science, Technology, Knowledge and Innovation, Chile and the National Agency of Research and Development (Agencia Nacional de Investigación y Desarrollo, ANID, Chile), for the financial support through FONDECYT Grant N° 11230400. Also, this paper was supported by the Vicerrectoría de Investigación y Doctorados de la Universidad San Sebastián, Chile USS-FIN-25- CNGI-06.

REFERENCES

[1] Forcellini D. Seismic fragility of tall buildings considering soil structure interaction (SSI) effects. Structures 2022;45:999–1011. https://doi.org/10.1016/j.istruc.2022.09.070.

[2] Forcellini D. A 3-DOF system for preliminary assessments of the interaction between base isolation (BI) technique and soil structure interaction (SSI) effects for low-rise buildings. Structures 2024;59:105803. https://doi.org/10.1016/j.istruc.2023.105803.

[3] De Risi R, Penna A, Simonelli AL. Seismic risk at urban scale: the role of site response analysis. Soil Dynamics and Earthquake Engineering 2019;123:320–36. https://doi.org/10.1016/j.soildyn.2019.04.011.

[4] Wu Y, Gao Z, Zhao M, Du X. Influence of structure-soil-structure interaction on seismic response and seismic migration performance of building structures. Journal of Building Engineering 2024;98:111101. https://doi.org/10.1016/j.jobe.2024.111101.

[5] Kanellopoulos C, Rangelow P, Jeremic B, Anastasopoulos I, Stojadinovic B. Dynamic structure-soil-structure interaction for nuclear power plants. Soil Dynamics and Earthquake Engineering 2024;181:108631. https://doi.org/10.1016/j.soildyn.2024.108631.

[6] Vicencio F, Torres-Olivares S, Flores EIS. Seismic Structure-Soil-Structure Interaction Between a Pair of Cross-Laminated Timber Buildings Under Seismic Loads, 2024, p. 3–21. https://doi.org/10.1007/978-3-031-53375-4_1.

[7] Vicencio F, Alexander NA. Seismic evaluation of Site-City interaction effects between city blocks. Front Built Environ 2024;10. https://doi.org/10.3389/fbuil.2024.1403642.

[8] Vicencio F, Alexander NA, Málaga-Chuquitaype C. Seismic Structure-Soil-Structure Interaction between inelastic structures. Earthq Eng Struct Dyn 2024. https://doi.org/10.1002/eqe.4076.

[9] Wang H, Lou M, Zhang R. Influence of presence of adjacent surface structure on seismic response of underground structure. Soil Dynamics and Earthquake Engineering 2017;100:131–43. https://doi.org/10.1016/j.soildyn.2017.05.031.

[10] Gan J, Li P, Liu Q. Study on Dynamic Structure-Soil-Structure Interaction of Three Adjacent Tall Buildings Subjected to Seismic Loading. Sustainability 2019;12:336. https://doi.org/10.3390/su12010336.

[11] Luque R, Bray JD. Dynamic soil-structure interaction analyses of two important structures affected by liquefaction during the Canterbury earthquake sequence. Soil Dynamics and Earthquake Engineering 2020;133:106026. https://doi.org/10.1016/j.soildyn.2019.106026.

[12] Han B, Chen S, Liang J. 2D dynamic structure-soil-structure interaction: A case study of Millikan Library Building. Eng Anal Bound Elem 2020;113:346–58. https://doi.org/10.1016/j.enganabound.2020.01.012.

[13] Aji HDB, Wuttke F, Dineva P. 3D structure-soil-structure interaction in an arbitrary layered half-space. Soil Dynamics and Earthquake Engineering 2022;159:107352. https://doi.org/10.1016/j.soildyn.2022.107352.

[14] Vicencio F, Torres-Olivares S, Miranda-Garnica M, Flores EIS, Málaga-Chuquitaype C. Seismic assessment of SSSI effects between adjacent Cross-Laminated Timber (CLT) buildings. Structures 2024;69:107318. https://doi.org/10.1016/j.istruc.2024.107318.

[15] Vicencio F, Cruz EF. A High Order Nonlinear Study to Evaluate the Seismic Response of Rotating Machines–Structure–Soil Foundation Systems. Journal of Earthquake Engineering 2021;25:2775–807. https://doi.org/10.1080/13632469.2019.1651422.

[16] Lu X, McKenna F, Cheng Q, Xu Z, Zeng X, Mahin SA. An open-source framework for regional earthquake loss estimation using the city-scale nonlinear time history analysis. Earthquake Spectra 2020;36:806–31. https://doi.org/10.1177/8755293019891724.

[17] Lu Y, Li B, Xiong F, Ge Q, Zhao P, Liu Y. Simple discrete models for dynamic structure-soil-structure interaction analysis. Eng Struct 2020;206:110188. https://doi.org/10.1016/j.engstruct.2020.110188.

[18] Vicencio F, Alexander NA, Saavedra Flores EI. A State-of-the-Art review on Structure-Soil-Structure interaction (SSSI) and Site-City interactions (SCI). Structures 2023;56:105002. https://doi.org/10.1016/j.istruc.2023.105002.

[19] Vicencio F, Alexander NA. Seismic Structure-Soil-Structure Interaction between a pair of buildings with consideration of rotational ground motions effects. Soil Dynamics and Earthquake Engineering 2022;163:107494. https://doi.org/10.1016/j.soildyn.2022.107494.

[20] Vicencio F, Alexander NA. Method to evaluate the dynamic structure-soil-structure interaction of 3-D buildings arrangement due to seismic excitation. Soil Dynamics and Earthquake Engineering 2021;141:106494. https://doi.org/10.1016/j.soildyn.2020.106494.

[21] Trombetta NW, Mason HB, Chen Z, Hutchinson TC, Bray JD, Kutter BL. Nonlinear dynamic foundation and frame structure response observed in geotechnical centrifuge experiments. Soil Dynamics and Earthquake Engineering 2013;50:117–33. https://doi.org/10.1016/j.soildyn.2013.02.010.

[22] Mason HB, Trombetta NW, Chen Z, Bray JD, Hutchinson TC, Kutter BL. Seismic soil-foundation-structure interaction observed in geotechnical centrifuge experiments. Soil Dynamics and Earthquake Engineering 2013;48:162–74. https://doi.org/10.1016/j.soildyn.2013.01.014.

[23] Trombetta NW, Benjamin Mason H, Hutchinson TC, Zupan JD, Bray JD, Kutter BL. Nonlinear Soil–Foundation–Structure and Structure–Soil–Structure Interaction: Engineering Demands. Journal of Structural Engineering 2015;141:1–12. https://doi.org/10.1061/(asce)st.1943-541x.0001127.

[24] Knappett JA, Madden P, Caucis K. Seismic structure–soil–structure interaction between pairs of adjacent building structures. Géotechnique 2015;65:429–41. https://doi.org/10.1680/geot.SIP.14.P.059.

[25] Qi S, Knappett JA. Influence of foundation type on seismic response of low-rise structures in liquefiable soil. Soil Dynamics and Earthquake Engineering 2020;128:105786. https://doi.org/10.1016/j.soildyn.2019.105786.

[26] Aldaikh H, Alexander NA, Ibraim E, Knappett J. Shake table testing of the dynamic interaction between two and three adjacent buildings (SSSI). Soil Dynamics and Earthquake Engineering 2016;89:219–32. https://doi.org/10.1016/j.soildyn.2016.08.012.

[27] Aldaikh H, Alexander NA, Ibraim E, Oddbjornsson O. Two dimensional numerical and experimental models for the study of structure-soil-structure interaction involving three buildings. Comput Struct 2015;150:79–91. https://doi.org/10.1016/j.compstruc.2015.01.003.